*Int. J. Morphol.,*
*43(6)*:2155-2162, 2025.

# Sex Estimation Based on Optical Channel Parameters from Computed Tomography Images with Machine Learning Algorithms

## Estimación del Sexo Basado en Medidas Radiológicas del Canal Óptico y Estructuras Circundantes Utilizando Algoritmos de Aprendizaje Automático

**Oguzhan Ozturk[1]; Oguzhan Harmandaoglu[1]; Seren Kaya[2]; Yusuf Secgin[3]; Deniz Senol[2]; Serdar Colakoglu[2] & Omer Onbas[4]**

**OZTURK, O.; HARMANDAOGLU, O.; KAYA, S.; SECGIN, Y.; SENOL, D.; COLAKOGLU, S. & ONBAS, O.** Sex estimation based on radiological measurements of the canalis opticus and surrounding structures using machine learning algorithms. *Int. J. Morphol., 43(6)*:2155-2162, 2025.

**SUMMARY:** The skull is one of the most dimorphic and anatomically informative bones for sex estimation and shows resistance to taphonomic processes. This study aims to estimate sex using machine learning (ML) algorithms based on morphometric measurements of the optic canal (OC)—a clinically significant canal within the sphenoid bone that transmits the optic nerve and ophthalmic artery. This retrospective study was conducted on CT from 260 adults (130 females and 130 males, aged 18–65). The images were obtained from the PACS archive of the Department of Radiology, Faculty of Medicine, Düzce University, covering the years 2019 to 2025. Sixteen bilateral morphometric parameters of the temporal bone were measured in axial and coronal planes. Data were analysed using various ML algorithms, and classification performance was compared. On the 20 % test set, ML models achieved over 81 % accuracy; Logistic Regression performed best with 90 %. In 10-fold cross-validation, all algorithms exceeded 74 %, with LR again reaching the highest at 89 %. Decision Tree yielded the lowest accuracy. SHapley Additive exPlanations (SHAP), which facilitates interpretable machine learning, revealed that the right-sided OC–midsagittal distance had the greatest predictive impact. Morphometric data from the OC provide high accuracy and strong potential for sex estimation. The study also highlights sex- and population-based variation in OC position. These findings may be relevant in clinical and forensic contexts, particularly in forensic anthropology, ophthalmology, and legal medicine.

**KEY WORDS: Sex estimation; Machine learning algorithms; Sphenoid bone; Optic canal.**

## INTRODUCTION

Human skeletal remains exhibit a variety of morphological traits that yield crucial insights into the identity of the deceased. Among these features, sex, age, and biological affinity are of primary importance. Sex determination during osteological analysis constitutes a foundational step in the process of human identification (Acar, 2014). Consequently, sex estimation is routinely employed in disciplines including archaeology, physical anthropology, and forensic medicine (Chovalopoulou *et al*., 2022). The process of sex estimation frequently necessitates interdisciplinary collaboration with the field of anatomy, which is indispensable for precise morphological interpretation (Mello-Gentil & Souza-Mello, 2022). While DNA technologies currently offer the highest level of reliability and precision, their high cost limits routine application. Consequently, osteometric methods, which are more cost-effective, are more commonly employed, and morphometric techniques are widely used to estimate sex based on skeletal elements (Giurazza *et al*., 2013). Sex estimation accuracy varies depending on the skeletal elements available, reaching up to 100 % with the complete skeleton, approximately 95 % with the pelvis, 92 % with cranial bones, and 80 % with long bones (Iscan & Steyn, 2013). Therefore, researchers frequently rely on the pelvis and cranial bones in sex estimation studies (Duric *et al*., 2005).

The sphenoid is a neurocranial bone composed of the body, greater wings, lesser wings, and the pterygoid processes. The junction between the body of sphenoid bone

[1] Kastamonu University, Catalzeytin Vocational School, Department of Physical Therapy and Rehabilitation, Kastamonu, Turkey.
[2] Düzce University, Faculty of Medicine, Department of Anatomy, Düzce, Turkey,
[3] Karabük University, Faculty of Medicine, Department of Anatomy, Karabük, Turkey.
[4] Düzce University, Faculty of Medicine, Department of Radiodiagnostics, Düzce.

Received: 2025-06-20 Accepted: 2025-09-03

and the lesser wing is referred to as the optic canal (OC). The OC transmits the optic nerve and the ophthalmic artery (Arıncı & Elhan, 2020). The OC is structurally composed of four walls. The superior wall is formed by either the anterior or posterior root of the lesser wing. The inferior wall arises from the posterior root of the lesser wing. The medial wall is formed by the body of the sphenoid bone, while the lateral wall consists of the anterior clinoid process (Yang *et al*., 2006). The[L1] OC has been described as an obliquely oriented cylindrical structure. Due to this configuration, its mediolateral dimension is greater than its superoinferior dimension. As a result, when progressing anteroposteriorly through the canal, the medial diameter is shorter than the lateral diameter (Abhinav *et al*., 2015).

Recent studies have demonstrated that artificial intelligence (AI) provides clinically significant insights into the prediction and treatment of diseases in the healthcare domain. Machine learning (ML), a subfield of AI, is categorised into three main types: supervised learning, unsupervised learning, and reinforcement learning. Supervised learning refers to algorithms that model input–output relationships; unsupervised learning uncovers patterns in previously unlabelled data; and reinforcement learning involves algorithms that associate inputs with desired outcomes (Petekci, 2021). Research employing ML methods has shown that different algorithms can produce varying outcomes (Bidmos *et al*., 2023). Although ML has traditionally been used in engineering, it has recently gained traction in healthcare as well (Da Costa Lewis, 2017). Through the use of ML techniques and data processing, sex estimation and individual identification can be efficiently performed in medical applications (Ogurtsova *et al*., 2017). Among ML algorithms, the Decision Tree (DT) builds a hierarchical structure composed of a root, decision nodes, branches, and leaves, enabling classification and regression tasks. Random Forest (RF) trains multiple DTs through randomisation, producing more stable and lower-variance predictions. Each DT in RF is trained using different subsets of the training dataset (Uddin *et al*., 2019). The Extra Trees Classifier (ETC), which shares similarities with RF, consists of numerous decision trees. However, ETC introduces greater randomness in the determination of split points and uses the entire learning dataset to grow each tree (Geurts *et al*., 2006). K-Nearest Neighbours (k-NN) is a commonly used classification algorithm that assigns classes based on the majority vote among the k nearest neighbours to the query sample (Uddin *et al*., 2022). Logistic Regression (LR), on the other hand, estimates the probability of a sample belonging to a specific class by applying a threshold to distinguish between two categories r (Uddin *et al*., 2019). Each ML algorithm has distinct advantages and limitations depending on the structure of the dataset and the specific nature of the target problem. These algorithms generate solutions by integrating statistical, probabilistic, and optimisation-based approaches, especially in the context of large and complex datasets (Uddin *et al*., 2019; Mavrogiorgou *et al*., 2022).

A review of the literature has revealed that, based on current knowledge, no study to date has utilised morphometric measurements obtained directly from the OC for the purpose of sex estimation. The aim of the present study is to estimate sex using measurements specific to the OC through machine learning algorithms. Given the limited body of research in this field, the present study has the potential to make an original contribution to the literature regarding the applicability of optic canal morphometry in sex determination.

## MATERIAL AND METHOD

**Ethical Approval and Study Design.** The study was approved by the Non-Interventional Local Ethics Committee of Düzce University, under decision number 2025/42. The study was designed as a retrospective investigation, and the radiological images used in the research were obtained from the Picture Archiving and Communication System (PACS) archive of the Department of Radiology at Düzce University.

In this retrospective study, a random selection of computed tomography (CT) images from 150 males and 150 females, acquired between 2019 and 2025, were reviewed. The final study sample included CT images from 130 males and 130 females aged between 18 and 65 years, in accordance with the exclusion criteria. The exclusion criteria were as follows: individuals outside the 18–65 age range; those with congenital cranial abnormalities; individuals with craniofacial fractures; and those with a history of cranial or facial surgery. The acquired images in Digital Imaging and Communications in Medicine (DICOM) format were imported into the Radiant DICOM Viewer (2023.1) software. Using the software's 3D Multiplanar Reconstruction (MPR) module, the images were reconstructed into three planes. Based on these images, the following bilateral axial measurements were obtained: OC length (midL), medial wall length (ML), lateral wall length (LL), OC–orbital width (OW), mid-canal width (MW), cranial canal width (CW), and OC–mid-sagittal line distance (OC–MSL). In addition, coronal images were used to measure the distance between the OC and the foramen rotundum (OC–FR) (Fig. 1).

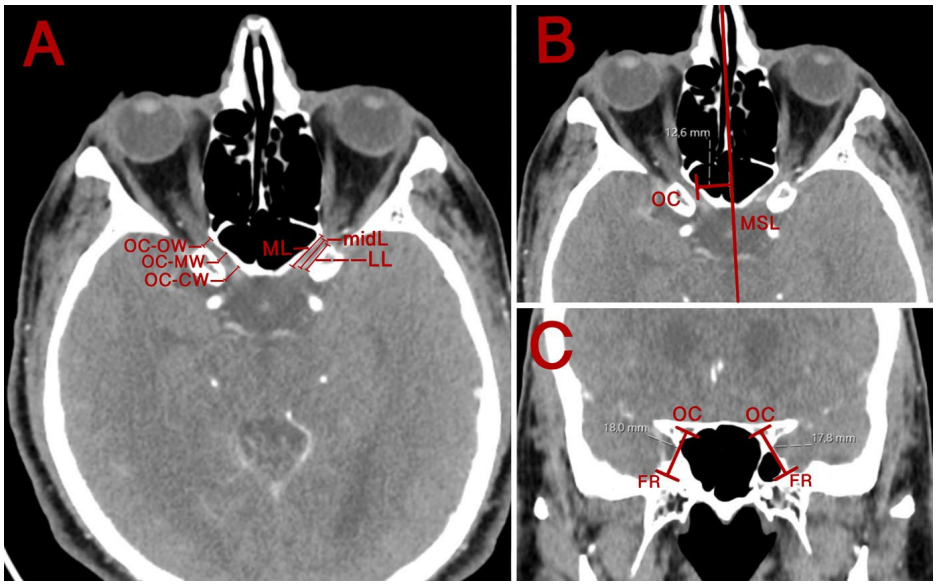


Fig. 1. Demonstration of measured parameters. A: Axial view showing measurements of the optic canal (OC) including orbital width (OC–OW), mid-canal width (OC–MW), cranial width (OC–CW), medial wall length (ML), lateral wall length (LL), and canal length (midL). B: Axial view showing the distance from the optic canal (OC) to the mid-sagittal line (MSL). C: Coronal view showing the distance between the optic canal (OC) and the foramen rotundum (FR).

**Machine Learning Algorithm Process.** In this study, the ML algorithms employed included LR, DT, ETC, RF, and k-NN. The algorithm analyses were conducted using the Python programming language on a personal computer with an i5 processor and 8 GB of RAM. The input layer of the models consisted of 16 parameters, while the output layer represented binary classification: male or female. For data splitting, both a 20 % test set and the 10-fold cross-validation method were applied. To assess the contribution of each parameter to the overall prediction, the SHapley Additive exPlanations (SHAP) method was implemented through the RF algorithm. The performance of the models was evaluated using the following metrics: Accuracy (Acc), Specificity (Spe), Sensitivity (Sen), and F1 Score (F1).

$$Acc = \frac{TP}{TP + FN + FP + TN}$$

$$\text{Sen} = \frac{TP}{TP+FN}$$

$$\text{Spe} = \frac{TN}{TN+FP}$$

$$\text{F1} = 2\frac{Spe \times Sen}{Spe+Sen}$$

Equation 1. (TP; True positive, TN; True negative, FP; False positive, FN; False negative).

**Basic Statistical Analyses.** The Anderson–Darling test was used to assess normality. For comparisons based on sex, the Two-Sample t-test was applied to normally distributed data, whereas the Mann–Whitney U test was used for non-normally distributed data. All statistical analyses were performed using Minitab 17 statistical software, with a significance level set at $p < 0.05$.

## RESULTS

The ages of the 130 female participants were 49 (25–63), while the ages of the male participants were 35 (18–63). It was found that the following parameters were normally distributed: right OC–midL, right OC–LL, right OC–CW, left OC–midL, left OC–ML, left OC–LL, left OC–MW, and left OC–CW. Among these, right OC–CW, left OC–MW, and left OC–CW showed statistically significant differences between sexes ($p < 0.05$) (Table I).

Table I. Descriptive statistics of normally distributed variables and their comparison by sex (Two-Sample t-test).

| Parameters | Sex | Mean ± SD | p |
|---|---|---|---|
| **Right OC-midL** | Male | 12.692±2.312 | 0.197 |
| | Female | 12.333±2.150 | |
| **Right OC-LL** | Male | 11.159±2.024 | 0.839 |
| | Female | 11.107±2.131 | |
| **Right OC-CW** | Male | 5.852±1.388 | **0.000** |
| | Female | 4.829±1.091 | |
| **Left OC-midL** | Male | 12.421±2.187 | 0.834 |
| | Female | 12.367±1.955 | |
| **Left OC-ML** | Male | 12.305±2.319 | 0.326 |
| | Female | 12.042±1.975 | |
| **Left OC-LL** | Male | 11.154±2.156 | 0.900 |
| | Female | 11.122±1.993 | |
| **Left OC-MW** | Male | 4.336±1.041 | **0.000** |
| | Female | 3.941±0.596 | |
| **Left OC-CW** | Male | 5.693±1.345 | **0.000** |
| | Female | 4.866±1.138 | |

It was found that, with the exception of the right OC–ML parameter, all other non-normally distributed parameters showed statistically significant differences between sexes ($p < 0.05$) (Table II).

Table II. Descriptive statistics of non-normally distributed variables and their comparison by sex (Mann–Whitney U test).

| Parameters | Sex | Median (Minimum–Maximum) | p |
|---|---|---|---|
| **Right OC-ML** | Male | 12.400 (7.900-19.400) | 0.252 |
| | Female | 12.150 (6.900-20.000) | |
| **Right OC-OW** | Male | 4.450 (1.900-8.400) | **0.000** |
| | Female | 3.500 (2.000-6.700) | |
| **Right OC-MW** | Male | 4.400 (1.900-7.400) | **0.003** |
| | Female | 4.000 (2.300-6.300) | |
| **Right OC-MSL** | Male | 11.400 (7.400-22.100) | **0.000** |
| | Female | 9.950 (6.900-14.100) | |
| **Right OC-FR** | Male | 19.400 (14.800-27.200) | **0.000** |
| | Female | 17.950 (13.500-22.900) | |
| **Left OC-OW** | Male | 4.300 (1.900-9.600) | **0.000** |
| | Female | 3.900 (2.200-7.100) | |
| **Left OC-MSL** | Male | 12.300 (8.300-20.700) | **0.000** |
| | Female | 10.800 (7.000-14.400) | |
| **Left OC-FR** | Male | 19.350 (13.500-27.100) | **0.000** |
| | Female | 17.75 (13.30-25.500) | |

As a result of the ML algorithms applied using a 20 % test set, the highest accuracy (Acc) was achieved with the Logistic Regression (LR) algorithm, with a value of 0.90 (Table III).

Table III. Performance metrics of machine learning models (20% test set).

| Algorithms | Accuracy (Acc) | Specificity (Spe) | Sensitivity (Sen) | F1 Score (F1) |
|---|---|---|---|---|
| LR | 0.90 | 0.91 | 0.91 | 0.90 |
| ETC | 0.85 | 0.85 | 0.85 | 0.85 |
| DT | 0.81 | 0.81 | 0.81 | 0.81 |
| RF | 0.83 | 0.83 | 0.83 | 0.83 |
| k-NN (n=5) | 0.87 | 0.87 | 0.86 | 0.86 |

Based on the Logistic Regression (LR) algorithm applied with a 20 % test set, 23 out of 24 male individuals and 24 out of 28 female individuals in the test set were correctly classified (Table IV).

The influence of each parameter on the overall prediction was analysed using the SHAP method, and the parameter with the greatest impact was found to be the right OC–MSL (Fig. 2).

Table IV. Confusion matrix of the Logistic Regression algorithm (20 % test set).

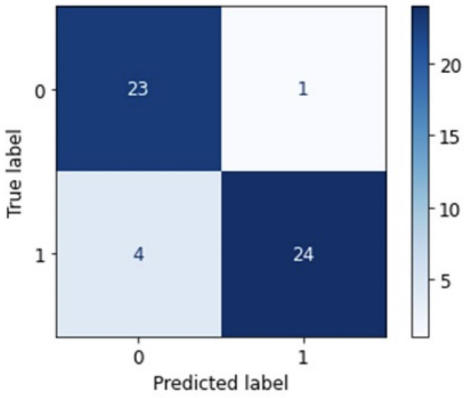


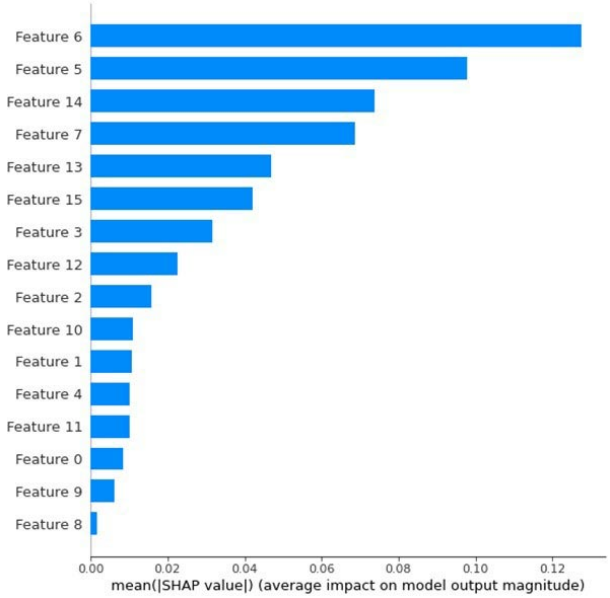


Fig. 2. SHAP summary plot of the Random Forest (RF) algorithm. (Feature: 0 – right optic canal length, 1 – right optic canal medial wall length, 2 – right optic canal lateral wall length, 3 – right optic canal–orbital width, 4 – right optic canal mid-canal width, 5 – right optic canal cranial width, 6 – right optic canal–mid-sagittal line distance, 7 – right optic canal–foramen rotundum distance, 8 – left optic canal length, 9 – left optic canal medial wall length, 10 – left optic canal lateral wall length, 11 – left optic canal–orbital width, 12 – left optic canal mid-canal width, 13 – left optic canal cranial width, 14 – left optic canal–mid-sagittal line distance, 15 – left optic canal–foramen rotundum distance.)

As a result of the ML algorithm analysis performed using 10-fold cross-validation, the highest accuracy (Acc) was achieved with the Logistic Regression (LR) algorithm, with a value of $0.89 \pm 0.049$ (Table V).

Table V. Performance metrics of machine learning models (10-fold cross-validation).

| Fold | LR | ETC | DT | RF | k-NN |
|---|---|---|---|---|---|
| 1 | 0.89 | 0.89 | 0.77 | 0.96 | 0.81 |
| 2 | 0.89 | 0.73 | 0.69 | 0.77 | 0.77 |
| 3 | 0.89 | 0.85 | 0.69 | 0.91 | 0.89 |
| 4 | 0.96 | 0.96 | 0.77 | 0.91 | 0.85 |
| 5 | 0.81 | 0.65 | 0.81 | 0.95 | 0.69 |
| 6 | 0.92 | 0.92 | 0.77 | 0.86 | 0.92 |
| 7 | 0.92 | 0.92 | 0.69 | 0.71 | 0.85 |
| 8 | 0.92 | 0.92 | 0.69 | 0.86 | 0.85 |
| 9 | 0.85 | 0.77 | 0.77 | 1.0 | 0.85 |
| 10 | 0.81 | 0.89 | 0.73 | 0.67 | 0.77 |
| Mean ± Standard Deviation | 0.89±0.049 | 0.85±0.100 | 0.74±0.045 | 0.86±0.110 | 0.83±0.067 |

LR-Logistic Regression; ETC-Extra Trees Classifier; DT-Decision Tree; RF-Random Forest; k-NN-k-Nearest Neighbours.

## DISCUSSION

In this study, we investigated the applicability of various OC measurements obtained from CT images for sex estimation using ML algorithms. Among the algorithms employed, LR demonstrated the highest accuracy rate at 90 %, while DT yielded the lowest performance with an accuracy of 81%. When the accuracy of the ML models was assessed using 10-fold cross-validation, LR again achieved the highest accuracy, at 89 %. The SHAP analysis revealed that the parameter with the greatest influence on sex prediction was the right OC–MSL.

In the field of forensic medicine, understanding the extent to which different bones contribute to sex estimation—one of the initial steps in establishing biological identity—is of critical importance. To this end, the literature contains numerous studies that focus on sex estimation using measurements of cranial structures and internal components exhibiting sexual dimorphism (Kaya *et al*., 2014; Toy *et al*., 2022; Senol *et al*., 2024). In this context, sex-related differences in orbitometric measurements have also been shown to play a significant role in forensic anthropology. These studies have examined the predictive value of parameters such as orbital height, width, intraorbital and extraorbital distances for sex estimation (Kaplanoglu *et al*., 2014; Kaya *et al*., 2014; Mani *et al*., 2020; Packirisamy *et al*., 2024). Although there are studies in the literature addressing the morphometric characteristics of the OC and comparing these between males and females (Hart *et al*., 2009; Inal *et al*., 2015; Kalthur *et al*., 2015; Sthapak *et al*., 2023), those studies have generally limited their analyses to the height and width of the orbital and cranial openings of the OC (Triantafyllou *et al*., 2024).

Machine learning algorithms are increasingly being employed in sex estimation studies due to their ability to analyze large datasets with high speed and accuracy in a meaningful manner (Secgin *et al*., 2022; Senol *et al*., 2024; Triantafyllou *et al*., 2024; Harmandaoglu *et al*., 2025). In the current literature, studies utilising ML algorithms for sex estimation based specifically on OC parameters are relatively limited. Triantafyllou *et al*. (2024) achieved an accuracy rate of 68 % using the RF algorithm based on orbital measurements. Their study, which included 35 male and 57 female dry skulls, assessed orbital length, width, intraorbital and extraorbital distances, as well as the height and width of the orbital and cranial openings of the optic canal. In our study, which involved a larger and more balanced sample, the performance and reliability of LR, DT, RF, ETC, and k-NN algorithms were compared. When compared with the study by Triantafyllou *et al*. (2024) only the width parameters of the orbital and cranial openings of the optic canal were found to overlap with those assessed in our CT-based investigation. In our findings, the accuracy rate obtained using the RF algorithm was 83 %, making it the second least accurate model after DT.

Adanir *et al*. (2022) reported the cranial opening width of the optic canal as 7.27±1.15 mm in their study based on CBCT images. In a cadaveric study, Demartini Jr. & Zanine (2021) measured the horizontal diameter of the cranial opening at a mean of 5.52 mm, the OC–MW at 5.20 mm, and the horizontal diameter of the orbital opening at 4.20 mm. Pirinç *et al*., measured the width of the orbital aperture as 3.7 mm and 3.88 mm on the right and left sides, respectively, in females, and 3.72 mm and 3.82 mm in males, and found no statistically significant difference between sexes. However, the OC-CW (optic canal–cranial wall) width was found to be 5.33 mm (right) and 5.36 mm (left) in females, and 5.87 mm (right) and 5.93 mm (left) in males, showing a significantly greater width in males on both sides. (Pirinc *et al*., 2023). Regarding the mid-canal width of the optic canal, no significant sex-based difference was observed; measurements were 4.94 mm and 5.16 mm in females and 5.09 mm and 5.03 mm in males, on the right and left sides respectively (Pirinc *et al*., 2023). In a study using CT imaging, Kalthur *et al*. (2015) reported cranial opening widths of 4.24 mm in females and 4.75 mm in males, and orbital width measurements of 2.8 mm and 3.25 mm,

respectively. Inal *et al*. (2015) measured the width of the optic canal at the sphenoid sinus level using coronalCT sections. They reported average values of 4.47 mm (right) and 4.86 mm (left) in males, and 4.36 mm (right) and 4.63 mm (left) in females. A statistically significant sex difference was observed for the left optic canal width (Inal *et al*., 2015). The width measurements of the optic canal at its orbital, cranial, and middle segments were found to be consistent with previous literature. Nonetheless, our study revealed a statistically significant difference between sexes.

In a study based on CT imaging, the lengths of the medial and lateral walls were measured and evaluated. The measurements in males were 10.86 mm (medial) and 9.3 mm (lateral), while in females they were 10.11 mm (medial) and 8.8 mm (lateral). Statistically significant sex-based differences were identified for all parameters (Kalthur *et al*., 2015). Similarly, another study that reported statistically significant differences between sexes found that the medial wall length was 10.27 mm (right) and 9.4 mm (left) in females, and 10.86 mm and 10.8 mm in males. The lateral wall length was measured as 9.5 mm (right) and 9.24 mm (left) in females, and 10.59 mm and 10.02 mm in males (Pirinc *et al*., 2023). In a CT-based study, Hart *et al*. (2009) reported the average medial wall length of the optic canal as 1.39 cm in females and 1.61 cm in males, and the lateral wall length as 1.00 cm and 1.13 cm, respectively. Both parameters showed statistically significant differences between sexes. In our study, however, no statistically significant sex differences were found in the medial and lateral wall lengths. This discrepancy may be attributed to racial or ethnic variation among the study populations.

In their cadaveric study, Demartini Jr. & Zanine (2021) reported the average length of the optic canal as 12.06 mm. Sthapak *et al*. (2023) found the optic canal length to be 9.72 mm (right) and 9.89 mm (left) in males, and 9.52 mm (right) and 9.24 mm (left) in females. In our study, the optic canal length was measured as 12.15 mm (right) and 12.04 mm (left) in females, and 12.40 mm (right) and 12.31 mm (left) in males.

In a CT-based study involving axial images of 200 individuals, the distance between the OC–MSL was evaluated, and—consistent with our findings—a statistically significant difference between sexes was reported for this parameter (Sthapak *et al*., 2023). In the aforementioned study, the distances were measured as 10.0 mm (right) and 9.70 mm (left) in females, and 10.78 mm (right) and 10.91 mm (left) in males. In our study, which produced similar results, the distance from the right optic canal to the mid-sagittal line was identified—via SHAP analysis—as the most influential parameter for sex classification, while the corresponding left-sided measurement ranked third in predictive importance.

In the CT-based study conducted by Inal *et al*. (2015) the distance between the OC and the foramen rotundum was measured as 20.34 mm (right) and 20.31 mm (left) in males, and 18.91 mm (right) and 18.80 mm (left) in females. Consistent with our findings, these distances were significantly greater in males, with the differences being statistically significant (Inal *et al*., 2015).

Kalthur *et al*. (2015) compared the morphometric measurements of the optic canal using both CT imaging and direct measurements on dry skulls. The cranial opening width was measured as 4.59 mm via CT and 5.48 mm via direct measurement. Similarly, the OC–OW was found to be 2.98 mm on CT and 4.74 mm through direct measurement. In the same study, the medial wall length was recorded as 10.63 mm (CT) and 9.10 mm (direct), while the lateral wall length was measured as 9.20 mm (CT) and 8.66 mm (direct) (Kalthur *et al*., 2015).

Although the findings of this study offer valuable contributions to the existing literature, several limitations must be acknowledged due to the methodological characteristics of the approaches employed. The ML algorithms used in our study yielded effective results in data-driven learning; however, each algorithm has its own methodological limitations in how it models the data. This study utilised and compared a range of different algorithms; nevertheless, the performance of other algorithms may be assessed in future studies. Although efforts were made to ensure a relatively large and balanced sample size, the current dataset may still be limited in its representativeness of the general population. Therefore, further research on broader and more diverse populations is warranted.

This study concluded that morphometric measurements of the OC, as well as its topographic position relative to the mid-sagittal plane, exhibit statistically significant differences between sexes and serve as effective parameters in sex estimation. In this study, which employed ML algorithms capable of producing rapid and reliable results, all models achieved classification accuracies exceeding 81% when applied to OC-based measurements. Although previous literature has established that morphometric features of the optic canal differ significantly between sexes, few studies have specifically examined the effectiveness of these parameters in sex prediction. Within this context, we believe that our study, which integrates both ML algorithms and a detailed assessment of OC morphometry, may offer a meaningful contribution to the existing body of research.

**OZTURK, O.; HARMANDAOGLU, O.; KAYA, S.; SECGIN, Y.; SENOL, D.; COLAKOGLU, S. & ONBAS, O.** Estimación del sexo basado en medidas radiológicas del canal óptico y estructuras circundantes utilizando algoritmos de aprendizaje automático. *Int. J. Morphol., 43(6)*:2155-2162, 2025.

**RESUMEN:** Los huesos del cráneoson los huesos con mayor dimorfismo e información anatómica para la estimación del sexo y muestra resistencia a los procesos tafonómicos. Este estudio tuvo como objetivo estimar el sexo utilizando algoritmos de aprendizaje automático (ML) basados en medidas morfométricas del canal óptico (CO)-un canal clínicamente significativo dentro del hueso esfenoides por donde transcurre el nervio óptico y la arteria oftálmica. Este estudio retrospectivo se realizó sobre TC de 260 adultos (130 mujeres y 130 hombres, de entre 18 y 65 años). Las imágenes se obtuvieron del archivo PACS del Departamento de Radiología de la Facultad de Medicina de la Universidad de Düzce, abarcando los años 2019 a 2025. Se midieron 16 parámetros morfométricos bilaterales del hueso temporal en planos axiales y coronales. Los datos se analizaron utilizando varios algoritmos ML y se comparó el rendimiento de la clasificación. En el conjunto de pruebas del 20 %, los modelos ML alcanzaron una precisión superior al 81%; la regresión logística obtuvo los mejores resultados, con un 90 %. En la validación cruzada de 10 veces, todos los algoritmos superaron el 74 %, siendo de nuevo la regresión logística la que alcanzó el 89 %. El árbol de decisión obtuvo la precisión más baja. SHapley Additive exPlanations (SHAP), que facilita el aprendizaje automático interpretable, reveló que la distancia OC-midsagital derecha tenía el mayor impacto predictivo. Los datos morfométricos del CO proporcionan una alta precisión y un fuerte potencial para la estimación del sexo. El estudio también pone de manifiesto la variación de la posición del CO en función del sexo y de la población. Estos hallazgos pueden ser relevantes en contextos clínicos y forenses, particularmente en antropología forense, oftalmología y medicina legal.

**PALABRAS CLAVE: Estimación del sexo; Algoritmos de aprendizaje automático; Hueso esfenoides; Canal óptico.**

## REFERENCES

Abhinav, K.; Acosta, Y.; Wang, W.-H.; Bonilla, L. R.; Koutourousiou, M.; Wang, E.; Synderman, C.; Gardner, P. & Fernandez-Miranda, J. C. Endoscopic endonasal approach to the optic canal: anatomic considerations and surgical relevance. *Neurosurgery, 11(Suppl. 3)*:431-45; discussion 445-6, 2015.

Acar, A. Yoncatepe toplumunda calcaneus ve talus kemiklerinden cinsiyet ve boy tahmini. *Anthropology, 28*:109-22, 2014.

Adanir, S. S.; Baks¸i, Y. E.; Beger, O.; Bahs¸i, I.; Kervanciog˘lu, P.; Yalçin, E. D. & Orhan, M. Evaluation of the cranial aperture of the optic canal on cone-beam computed tomography images and its clinical implications for the transcranial approaches. *J. Craniofac. Surg., 33(6)*:1909-13, 2022.

Arıncı, K. & Elhan, A. *Anatomi.* Vol. 1. Ankara, Günes Tıp Kitapevleri, 2020.

Bidmos, M. A.; Olateju, O. I.; Latiff, S.; Rahman, T. & Chowdhury, M. E. H. Machine learning and discriminant function analysis in the formulation of generic models for sex prediction using patella measurements. *Int. J. Legal Med., 137(2)*:471-85, 2023.

Chovalopoulou, M. E.; Valakos, E. & Nikita, E. Skeletal sex estimation methods based on the Athens Collection. *Forensic Sci., 2(4)*:715-24, 2022.

Da Costa Lewis, N. M*achine Learning Made Easy with R: An Intuitive Step by Step Blueprint for Beginners*. CreateSpace Independent Publishing Platform, 2017.

Demartini Jr., Z. & Zanine, S. C. Microanatomic study of the optic canal. *World Neurosurg., 155*:e792-e796, 2021.

Duric, M.; Rakocevic, Z. & Donic, D. The reliability of sex determination of skeletons from forensic context in the Balkans. *Forensic Sci. Int., 147(2-3)*:159-64, 2005.

Geurts, P.; Ernst, D. & Wehenkel, L. Extremely randomized trees. *Mach. Learn., 63(1)*:3-42, 2006.

Giurazza, F.; Schena, E.; Del Vescovo, R.; Cazzato, R. L.; Mortato, L.; Saccomandi, P.; Paternostro, F.; Onofri, L. & Zobel, B. B. Sex determination from scapular length measurements by CT scan images in a Caucasian population. *Proc. Annu. Int. Conf. IEEE Eng. Med. Biol. Soc., 2013*:1632-5, 2013.

Harmandaoglu, O.; Seçgin, Y.; Kaya, S.; Öztürk, O.; S¸enol, D. & Önbas¸, Ö. Gender classification using parameters obtained from the dens axis with machine learning algorithms and multilayer perceptron classifier. *Iran. Red Crescent Med. J., 27(1)*, 2025.

Hart, C. K.; Theodosopoulos, P. V. & Zimmer, L. A. Anatomy of the optic canal: a computed tomography study of endoscopic nerve decompression. *Ann. Otol. Rhinol. Laryngol., 118(12)*:839-44, 2009.

Inal, M.; Muluk, N. B.; Arikan, O. K. & S¸ahin, S. Is there a relationship between optic canal, foramen rotundum, and vidian canal? *J. Craniofac. Surg., 26(4)*:1382-8, 2015.

Iscan, M. Y. & Steyn, M. *The Human Skeleton in Forensic Medicine.* Springfield (IL), Charles C. Thomas Publisher, 2013.

Kalthur, S.; Periyasamy, R.; Kumar, S.; Gupta, C. & D'souza, A. S. A morphometric evaluation of the optic canal: comparative study between computerized tomographic study and direct anatomic study. *Saudi J. Med. Med. Sci., 3(3)*:204, 2015.

Kaplanoglu, V.; Kaplanoglu, H.; Toprak, U.; Parlak, I˙. S.; Tatar, I˙. G.; Deveer, M. & Hekimoglu, B. Anthropometric measurements of the orbita and gender prediction with three-dimensional computed tomography images. *Folia Morphol. (Warsz)., 73(2)*:149-52, 2014.

Kaya, A.; Uygun, S.; Eraslan, C.; Akar, G. C.; Kocak, A.; Aktas, E. & Govsa, F. Sex estimation: 3D CTA-scan based on orbital measurements in Turkish population. *Rom. J. Leg. Med., 22(4)*:257-62, 2014.

Mani, S. M.; Ahamed, Y. S.; Ambiga, P.; Ramalingam, V.; Sivaraman, G. & Balan, N. Evaluation of orbital morphometry using 3D computed tomographic images in biological sex determination: a retrospective study. *J. Indian Acad. Oral Med. Radiol., 32(4)*:390, 2020.

Mavrogiorgou, A.; Kiourtis, A.; Kleftakis, S.; Mavrogiorgos, K.; Zafeiropoulos, N. & Kyriazis, D. A catalogue of machine learning algorithms for healthcare risk predictions. *Sensors (Basel), 22(22)*:8615, 2022.

Mello-Gentil, T. & Souza-Mello, V. Contributions of anatomy to forensic sex estimation: focus on head and neck bones. *Forensic Sci. Res., 7(1)*:11-23, 2022.

Ogurtsova, K.; da Rocha Fernandes, J. D.; Huang, Y.; Linnenkamp, U.; Guariguata, L.; Cho, N. H.; Cavan, D.; Shaw, J. E. & Makaroff, L. E. IDF Diabetes Atlas: global estimates for the prevalence of diabetes for 2015 and 2040. *Diabetes Res. Clin. Pract., 128*:40-50, 2017.

Packirisamy, V.; Aljarrah, K. & Nayak, S. B. Morphometric evaluation of the orbital region for sex determination in a Saudi Arabian population using 3DCT images. *Anat. Sci. Int., 99(1)*:118-26, 2024.

Petekci, A. R. *Teorik Olarak Makine Ögrenimi*. Kitapyurdu Dogrudan Yayıncılık, 2021.

Pirinc, B.; Fazliogullari, Z.; Koplay, M.; Unver Dogan, N. & Karabulut, A. K. Morphometric and morphological evaluation of the optic canal in three different parts in MDCT images. *Int. Ophthalmol., 43(8)*:2703-20, 2023.

Secgin, Y.; Oner, Z.; Turan, M. K. & Oner, S. Gender prediction with the parameters obtained from pelvis computed tomography images and machine learning algorithms. *J. Anat. Soc. India, 71(3)*:204, 2022.

Senol, D.; Secgin, Y.; Harmandaoglu, O.; Kaya, S.; Duman, S. B. & Oner, Z. Gender prediction using cone-beam computed tomography measurements from foramen incisivum: application of machine learning algorithms and artificial neural networks. *J. Anat. Soc. India, 73(2)*:152, 2024.

Sthapak, E.; Pasricha, N.; Narayan, S.; Gaharwar, A. & Bhatnagar, R. Optic canal: a CT-based morphometric study in north Indian population. *Egypt. J. Neurosurg., 38(1)*:46, 2023.

Toy, S.; Secgin, Y.; Oner, Z.; Turan, M. K.; Oner, S. & Senol, D. A study on sex estimation by using machine learning algorithms with parameters obtained from computerizedtomography images of the cranium. *Sci. Rep., 12(1)*:4278, 2022.

Triantafyllou, G.; Botis, G. G.; Piagkou, M.; Papanastasiou, K.; Tsakotos, G.; Paschopoulos, I.; Matsopoulos, G. K. & Papadodima, S. Sex estimation through orbital measurements: a machine learning approach for forensic science. *Diagnostics, 14(24)*:2773, 2024.

Uddin, S.; Haque, I.; Lu, H.; Moni, M. A. & Gide, E. Comparative performance analysis of k-nearest neighbour (KNN) algorithm and its different variants for disease prediction. *Sci. Rep., 12(1)*:6256, 2022.

Uddin, S.; Khan, A.; Hossain, M. E. & Moni, M. A. Comparing different supervised machine learning algorithms for disease prediction. *BMC Med. Inform. Decis. Mak., 19(1)*:281, 2019.

Yang, Y.; Wang, H.; Shao, Y.; Wei, Z.; Zhu, S. & Wang, J. Extradural anterior clinoidectomy as an alternative approach for optic nerve decompression: anatomic study and clinical experience. *Neurosurgery, 59(4 Suppl. 2)*:ONS253-62; discussion ONS262, 2006.

Corresponding author:
Asst. Prof. Dr. Yusuf Secgin
Department of Anatomy
Faculty of Medicine
Karabük University
Karabük
TURKEY

E-mail: yusufsecgin@karabuk.edu.tr